

Electrochemical Evaluation of the Mechanism of Acetylcholinesterase Inhibition Based on an Electrodeposited Thin Film

Hongxia Zhang^{1,2}, Jiawang Ding^{1,*}, Dan Du³

¹Key Laboratory of Coastal Environmental Processes and Ecological Remediation, Yantai Institute of Coastal Zone Research (YIC), Chinese Academy of Sciences (CAS); Shandong Provincial Key Laboratory of Coastal Environmental Processes, YICCAS, Yantai, Shandong 264003, P. R. China

²University of Chinese Academy of Sciences, Beijing 100049, P. R. China

³Key Laboratory of Pesticide and Chemical Biology of Ministry of Education, Huazhong Normal University, Wuhan 430079, PR China

*E-mail: jwding@mail.ccnu.edu.cn

Received: 9 November 2014 / Accepted: 14 December 2014 / Published: 30 December 2014

An interface embedded gold nanoparticles in sol-gel thin film was constructed by one-step electrochemical deposition. Acetylcholinesterase (AChE) was physically absorbed onto the interface to form a thin enzymatic layer. The proposed thin enzymatic layer, having kinetics similar to that of the enzyme in solution, provides an ideal sensing platform to electrochemically evaluate the chemical mechanism of enzyme inhibition. Lineweaver-Burk plot and surface plasmon resonance confirmed that the inhibition of AChE by malathion followed an irreversible mechanism and was a mixed type of competitive and noncompetitive. On the contrary, the degrees of inhibition by Pb^{2+} and Fe^{3+} were independent of the incubation time and the AChE concentrations, showing the reversibility of the inhibition. Furthermore, UV-vis absorption spectra indicated that the AChE mediated the hydrolysis of acetylthiocholine to yield a reducing agent thiocholine that reduced Fe^{3+} to Fe^{2+} and Fe^{2+} presented an effect of activation. To meet the demand of the biosensor design, we further investigated the relationship between inhibition percentage and both incubation time and inhibitor concentration. The enzyme's sensitivity to solvent effects and reactivation of the biosensor were also evaluated. It is anticipated that a rapid evaluation of the chemical mechanism of AChE inhibition could pave the way to rationally design biosensors and new compounds, as candidates for the treatment of Alzheimer's disease and pesticides.

Keywords: acetylcholinesterase; biosensor; inhibition mechanism, electrochemical, electrodeposition

1. INTRODUCTION

The importance of acetylcholinesterase (AChE) in the transmission of nerve impulses and the consequences of its inactivation, mainly with certain nerve gases, pesticides and heavy metal are well known [1]. In recent years, biosensors based on the principle of AChE inhibition have been extensively reported for a range of analytes, such as pesticides, drugs, and neurotoxins [2-6].

Despite the interest in designing AChE inhibition-based biosensors, there are confusions in the literature over what type of responses or quantitative relationships are expected from the immobilized enzyme biosensors [7]. Therefore, the understanding of the chemical mechanism of AChE inhibition and the quantitative relationship between inhibition percentage and both incubation time and inhibitor concentration is essential for biosensor design. In addition, the understanding of selected potent AChE inhibitors mechanism of action is key information to rationally design new compounds, as candidates for the treatment of Alzheimer's disease and pesticide [8]. So far, a variety of approaches to identify AChE inhibitors and to evaluate the inhibition mechanisms have been described [1,6,8]. UV-Vis spectrophotometry is one of the most widely used tool to investigate the inhibition mechanism of AChE using Ellman's reagent [6,9]. As an alternative, the electrochemical approach could provide new information in studying the process of enzyme inactivation using an enzyme electrode. Stoytcheva's group has exploited the process of inhibition of the immobilized cholinesterases by chlorofos and some inorganic ions such as As^{3+} , Hg^{2+} and F^- [10-13]. We have shown that electrochemical AChE biosensor can be used for pesticide and medicine sensitivity test [14,15].

On the basic of the numerous studies reported before, the kinetics of the inhibition depends strongly on the biosensor configuration. In the case of a thin enzymatic layer, the kinetics observed is similar to that of the enzyme in solution [16]. Therefore, a key challenge to the development of sensitive and stable biosensors for evaluating the chemical mechanism of AChE inhibition comes from the effective immobilization of AChE to solid electrode surface [17]. So far, immobilization techniques including covalent fixing or physical adsorption of AChE directly onto the surface of electrodes have been reported in the literature [10,12]. However, these protocols may affect the stability, the longevity and the sensitivity of the electrochemical biosensor and subsequently the study on the chemical mechanism of AChE inhibition. Therefore, new immobilization techniques, which can offer simplicity of preparation without covalent modification, flexibility in controlling film components, and geometry and minimal of losing enzyme activities, are needed.

Recently, electrochemical deposition has been proved to be an effective method for the immobilization of enzyme due to the formation of sol-gel films [18]. The proposed immobilization procedure is based on a local electrochemically induced pH modulation which induces the film formation [19]. Chitosan, as an excellent candidate for enzyme immobilization, has been electrochemically deposited onto electrodes for biosensor design [20,21]. However, the chitosan hydrogel experiences considerable swelling because of the water influxes. Sol-gel derived silicate network is also an attractive matrix for enzyme immobilization. Previous reports have shown that an elegant combination of electrochemistry with the sol-gel process can provide an attractive way for the immobilization of biological entities without preventing their activity [22,23]. The main problem

associated with such membrane is the difficulty to maintain the long-term stability due to the detachment of the film.

In this work, we try to use an electrodeposited thin film including sol-gel-derived silicate network (SiSG), gold nanoparticles (AuNPs) and chitosan for electrochemical study of the mechanism of AChE inhibition. Chitosan with excellent film-forming ability, high permeability and good adhesion was added into the sol-gel derived silicate network to avoid the detachment of the film. Moreover, AuNPs are incorporated into the sol-gel to facilitate electron transfer [24-26]. The main motivation of the present work was to use electrodeposited sol-gel thin film to replace precious covalent fixing or directly physical adsorption. It will be shown that AChE can keep its enzymatic activity in the electrodeposited thin AuNPs-SiSG films. The proposed AChE biosensor could be employed as a sensing platform to evaluate the chemical mechanism of acetylcholinesterase inhibition by malathion or metal ions, related with inhibitor concentration, incubation time, and organic solvents.

2. EXPERIMENTAL

2.1. Reagents

Acetylthiocholine chloride (ATCl) and acetylcholinesterase AChE (Type C3389, 500 U/mg from electric eel) were purchased from Sigma-Aldrich (St. Louis, USA) and used as received. Tetrathoxysilane (TEOS) was obtained from international laboratory (USA). 5,5'-bithiobis-2-nitrobenzoate (DTNB) was obtained from Alfa Aesar, 1,10-phenanthroline and $\text{HAuCl}_4 \cdot 4\text{H}_2\text{O}$ (Au% > 48%) were obtained from TreeChem.co (Shanghai, China). Malathion was obtained from AccuStandard (USA). Iron(III) and lead was selected from Shanghai Chemical Company. Chitosan (95% deacetylation), acetone, ethanol, phosphate buffer solution (0.02 M PBS, pH 7.0) and other reagents were of analytical reagent grade. All solutions were prepared with double distilled water.

2.2. Biosensor design

Gold disk electrode (1.0 mm in diameter) was used for the electrochemical measurement. Before modification, the gold electrode was pretreated as described before [27].

The solution of 17-nm-diameter AuNPs was prepared according to the literature [28] and stored in a brown bottle at 4 °C. A homogenous AuNPs-SiSG composite was prepared by mixing 50 μL of TEOS, 20 μL of ethanol, 150 μL of AuNPs, 600 μL of 0.5 mg/mL chitosan solutions (final concentration 0.3 %). Its pH was adjusted to 7.0-8.0 using 95 μL 0.1 M NaOH solution. The mixture was put into the electrochemical cell where electrodeposition was performed at -1.2 V at room temperature for typically 10 s [23,29]. The electrodes were rinsed with water, dried for 60 min in air and stored at 4 °C when not in use. For biosensor design, AChE was cast on the electrode. After evaporation of water, it was coated with 4.0 μL AChE solution (100 mU) to obtain the AChE-AuNPs-SiSG/Au.

2.3. Electrochemical evaluation of inhibition mechanisms

Electrochemical measurements were performed with a CHI 660C electrochemical workstation. A conventional three-electrode electrochemical cell was used consisting one of the above electrodes, a Pt-wire auxiliary electrode, and an Ag/AgCl (3 M KCl) reference electrode.

All the measurements were carried out in PBS buffer solution (pH 7.0) by cyclic voltammetry from 0.3 to 1.0 V. The heights of the current peak corresponding with the reduction of thiocholine at 0.94 V was used a quantitative measurement of the enzyme activity.

For the measurements of inhibitors, the pretreated AChE-AuNPs-SiSG/Au was first immersed in the PBS solution containing different concentrations of standard inhibitor solution for a fixed time, and then transferred to the electrochemical cell of 1.0 mL pH 7.0 PBS containing 0.3 mM ATCl to study the electrochemical response by cyclic voltammetry (CV). The inhibition percentage was calculated as follows:

$$\text{Inhibition (\%)} = 100 \times (i_{\text{P, control}} - i_{\text{P, exp}}) / i_{\text{P, control}}$$

Where $i_{\text{P, control}}$ and $i_{\text{P, exp}}$ were the peak currents of ATCl on AChE-AuNPs-SiSG/Au without and with inhibitor, respectively.

2.4. SPR measurements

SPR measurements were conducted using a single-channel Autolab SPRINGLE instrument (Eco Chemie, The Netherlands). The sensor chip has 50 nm thick gold layer and 5 nm titanium sublayer as the adhesive layer, attached to the prism using an index-matching oil ($n_d^{25^\circ\text{C}} = 1.45$). Binding curves were acquired and processed with the associated software. UV spectra were recorded using a UV-2501 spectrophotometer (Shimadzu; Kyoto Japan).

3. RESULTS AND DISCUSSION

3.1. Preparation and electrochemical characterization of AChE-AuNPs-SiSG/Au

Previous report has shown that immobilized hemoglobin or myoglobin in so-gel-derived thin films can enhance its peroxidase properties compared to solution [23]. In this work, AuNPs doped silicate-chitosan network, which served as the interfacial template for immobilization of AChE, was constructed by one-step electrodeposition. The electrodeposited sol-gel thin film is an ideal sensing platform to electrochemically evaluate the chemical mechanism of enzyme inhibition. The cyclic voltammograms of AChE-AuNPs-SiSG/Au was investigated (Fig. 1). In the presence of 0.3 mM ATCl, an irreversible oxidation peak at 940 mV (curve g) was observed for AChE-AuNPs-SiSG/Au, while no detectable signal was found for AuNPs-SiSG/Au (curve c). Moreover, control experiments revealed that the peak is caused by the oxidation of thiocholine (the hydrolysis product of ATCl), which is catalyzed by the immobilized AChE (curve a, b). The enzyme exhibits a fast response and high affinity to its substrate. Moreover, peak currents were found to be directly proportional to the

potential scan rate from 10 to 200 mV s^{-1} , indicating a thin layer electrochemical behavior [23]. The produced current by thiocholine can be used for quantification of the enzyme activity, which reflects the biological effect of an organophosphate pesticide or other inhibitors involved in the inhibition action [30].

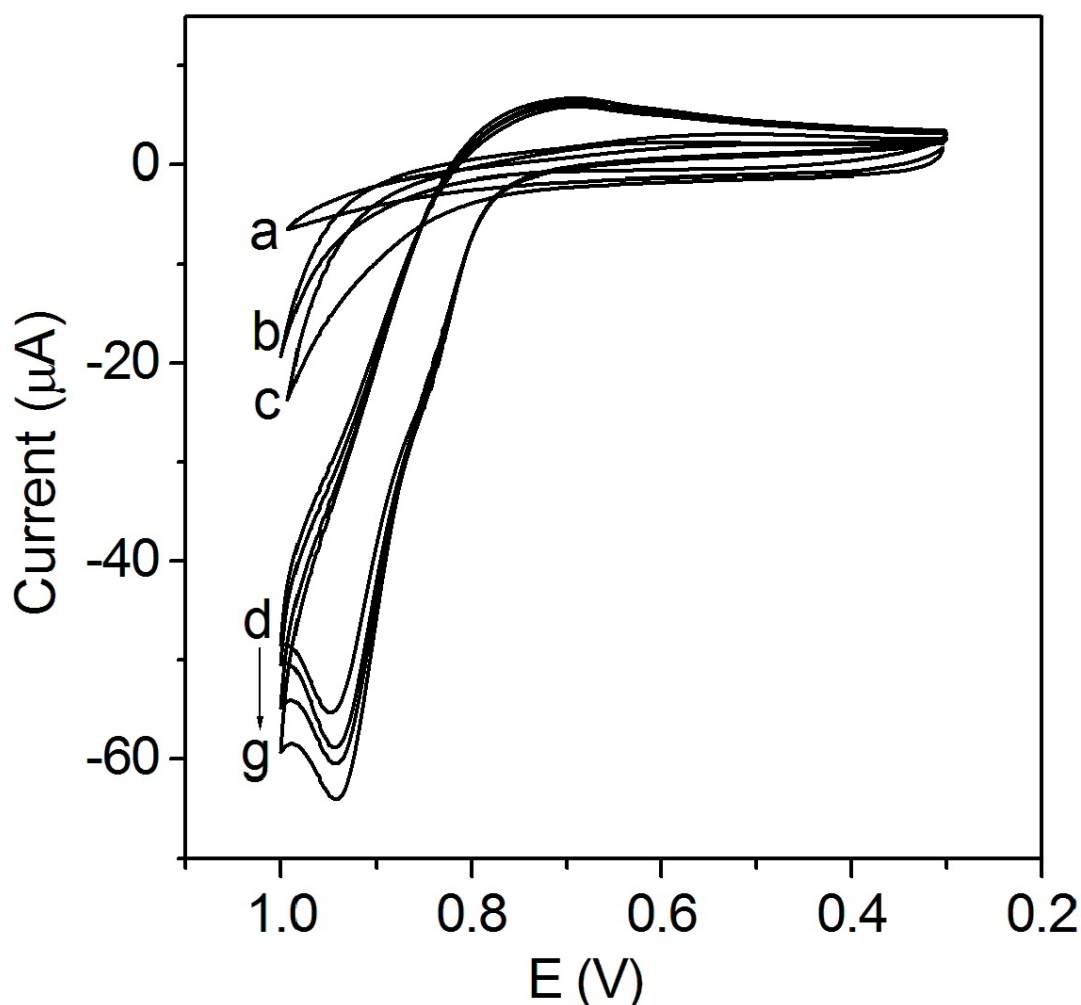


Figure 1. Cyclic voltammograms of (a) AuNPs-SiSG/Au; (b) AChE-AuNPs-SiSG/Au in pH 7.0 PBS; (c) AuNPs-SiSG/Au (g) AChE-AuNPs-SiSG/Au in pH 7.0 PBS containing 0.3 mM ATCl and AChE-AuNPs-SiSG/Au in pH 7.0 PBS containing 0.3 mM ATCl after immersed in (d) $0.1 \mu\text{g mL}^{-1}$ malathion solution (e) $50 \mu\text{g mL}^{-1} \text{Fe}^{3+}$ and (f) $50 \mu\text{g mL}^{-1} \text{Pb}^{2+}$ for 10 min.

Herein, malathion, iron(III) and lead were selected as model inhibitors. As shown in Fig. 1, all the selected inhibitors display inhibition to AChE. The AChE-AuNPs-SiSG/Au could be used to evaluate the inhibition mechanisms.

3.2. Reversibility of the AChE inhibition by malathion and metal ions.

It is essential to evaluate the inhibitory mechanism in order to determine the suitability of AChE for a screening assay [9]. We studied whether the inhibition is of a reversible or irreversible

type. In this article, the degree of inhibition at a fixed concentration of malathion ($1 \mu\text{g mL}^{-1}$), Fe^{3+} ($50 \mu\text{g mL}^{-1}$) and Pb^{2+} ($50 \mu\text{g mL}^{-1}$) using various concentrations of immobilized AChE was first investigated. The enzyme concentrations used for this experiment were 0.05, 0.1 and 0.2 mU mL^{-1} . For malathion, the degrees of inhibition obtained were 50.4, 31.51 and 21.29 % respectively. Obviously, a higher percentage of inhibition is observed with lower enzyme concentration, which indicated that the inhibition of AChE by malathion follows a irreversible mechanism [16,31]. It should be noted that the dissociation constant for the initial reversible enzyme inhibitor-complex is ca 10^{-5} M^{-1} [32]. Therefore, malathion may show a weak reversible inhibition at lower concentrations. The degrees of inhibition obtained were, 8.58, 8.60, 8.55 % for Fe^{3+} , and 15.33, 15.42, 15.47 % for Pb^{2+} . The inhibition of AChE with metal ions may be due to their capacity to form histidine complexes. The dissimilarity in the inhibition effect of Fe^{3+} , and Pb^{2+} could be explained with the different stability of the formed complexes [33]. Since there are no changes in degree of inhibition, the inhibition of AChE by metal ions follows a reversible mechanism. These results are consistent with the spectrophotometric method of Ellman [34].

3.3. Study of the type of AChE inhibition

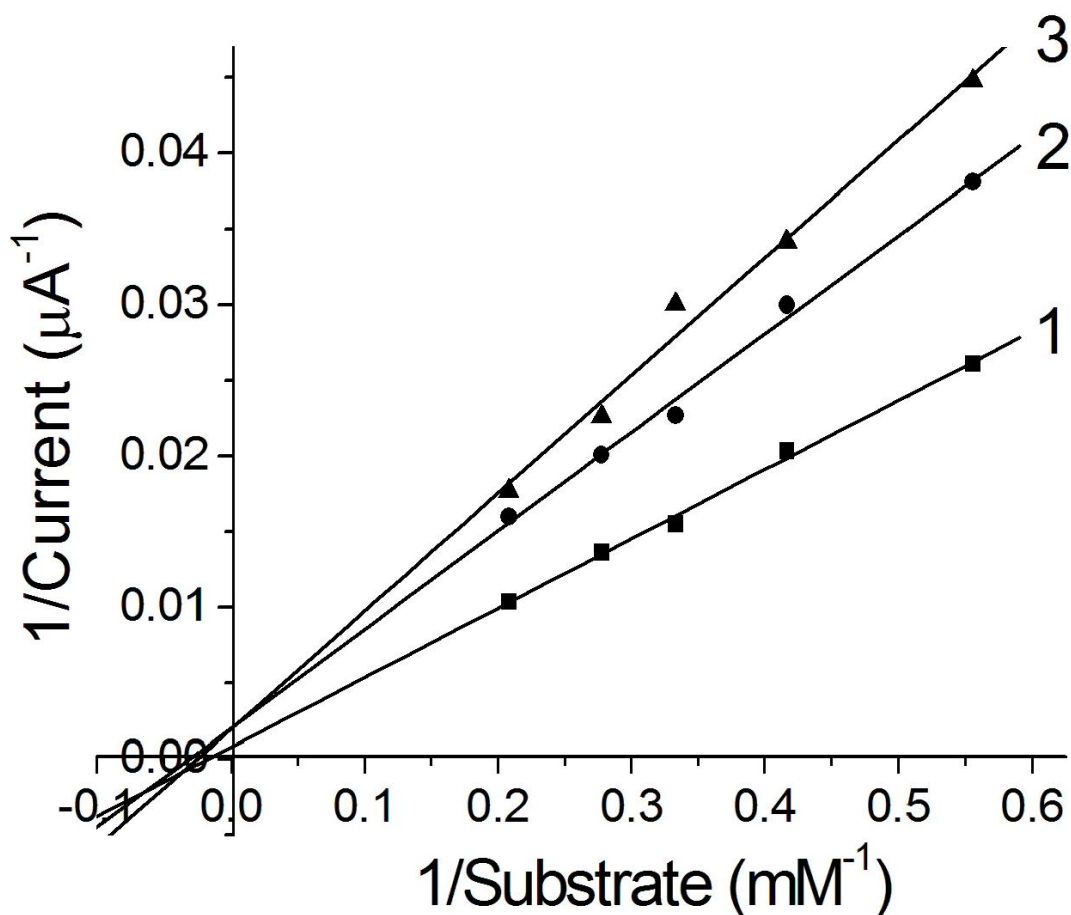


Figure 2. Lineweaver-Burk plot representing reciprocals of the current vs ATCl concentration without (1) and with (2) $1 \mu\text{g mL}^{-1}$ and (3) $10 \mu\text{g mL}^{-1}$ malathion.

To fully understand the inhibition mechanisms, experiments were then performed to evaluate whether the inhibition was competitive, uncompetitive, noncompetitive, or mixed. AChE activity was determined using ATCl concentrations over the range from 1.8 mM to 9 mM either in the absence or presence of fixed malathion ($1 \mu\text{g mL}^{-1}$ and $10 \mu\text{g mL}^{-1}$) or metal ions concentrations ($50 \mu\text{g mL}^{-1}$).

As shown in the Lineweaver-Burk plot (Fig. 2), the lines are not parallel and thus the inhibition is not uncompetitive. In addition, the lines pass through different points on the ordinate and intersect at a point slightly displaced from the abscissa in the second quadrant. Therefore, the AChE inhibition by malathion is a mixed type of competitive and noncompetitive [9]. The inhibition of AChE by metal ions was also evaluated according to the Lineweaver-Burk plots. As can be seen from Fig. 3, the inhibition had a reversible and a noncompetitive character for metal ions [9].

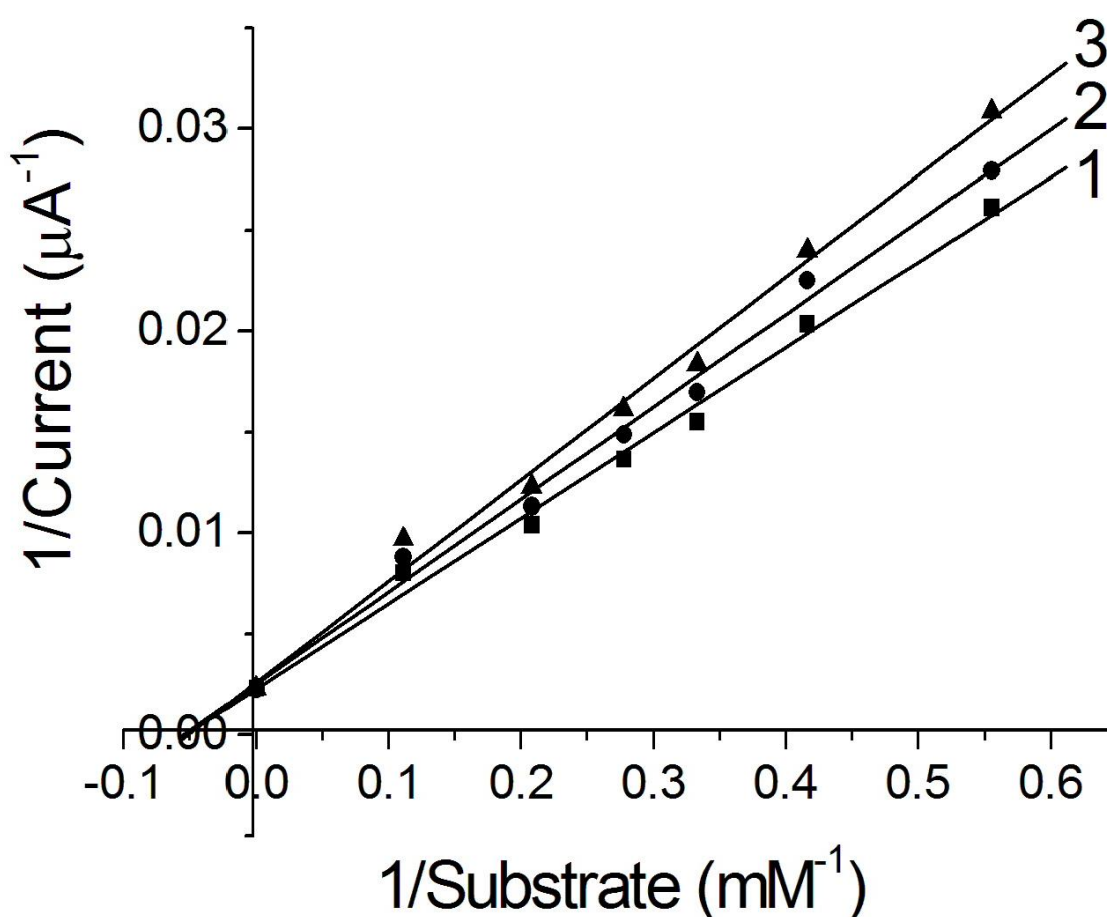


Figure 3. Lineweaver-Burk plot representing reciprocals of the current vs ATCl concentration without (1) and with $50 \mu\text{g mL}^{-1}$ (2) Fe^{3+} and (3) Pb^{2+} .

SPR has emerged as a powerful tool for real-time monitoring small changes in a solid/liquid interface. In this article, SPR was used to investigate the type of AChE inhibition. The performance of the AChE assay, consisting of surface pre-treatment (1), sample injection (2) and washing step (3), is documented by the sensorgram presented in Fig. 4. The gold surface was modified with AChE-AuNPs-SiSG. Subsequently a sample containing malathion (c) or a mixture of ATCl and malathion (b) was injected and allowed to bind to the AChE on the gold surface. The differences between baseline

values before and after sample injection were used for determination of the amount of bound malathion. When malathion was introduced, the SPR resonance angle shifts about 78 m° (108 m° - 30 m°), which is obviously larger than that of a mixture of ATCl and malathion was introduced (resonance angle shifts about 5 m° (53 m° - 48 m°)). Thus, it can be infer that excess of ATCl stopped the interaction of the enzyme and the inhibitor due to the formation of an enzyme-substrate complex which could not react with the pesticide [31]. Therefore, there do exist some extent competition between ATCl and malathion. The results are in good agreement with the results from Lineweaver-Burk plot mentioned above.

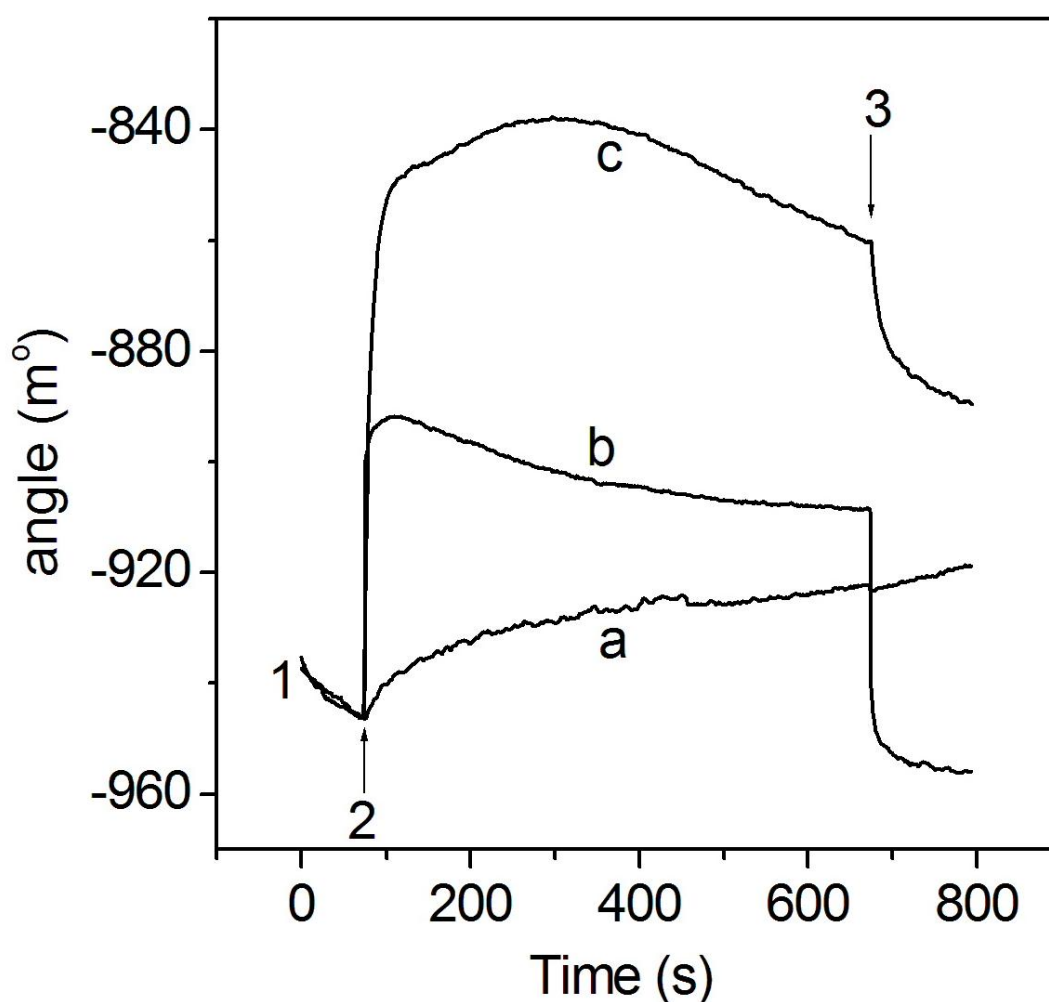


Figure 4. SPR sensorgram responses to the interaction between enzyme and substrate. The gold surface was modified with AChE-AuNPs-SiSG; subsequently a sample containing malathion (c) or a mixture of ATCl and malathion (b) was injected and allowed to bind to the AChE on the gold surface. (1), (2) and (3) represent the pre-treatment, sample injection and washing step, respectively.

3.4. The relationship between inhibition percentage and incubation time

Incubation time is a very important parameter for enzyme-inhibition based biosensing systems. For irreversible inhibition, a low detection limit can be obtained with a longer incubation time. Fig. 5

shows the experimental results obtained from malathion inhibition. A linear relationship between inhibition percentage and the square root of the incubation time were obtained. Our result is in good agreement with a theoretical model for immobilized enzyme inhibition biosensors, which predicts that the percentage of inhibited enzyme, after exposure to an inhibitor, is linearly related to both the inhibitor concentration and the square root of incubation time ($t^{1/2}$) [35].

Then, the effect of incubation time was also evaluated between 0 and 20 min for metal ions, obtaining a degree of inhibition equal to 15.42 % for Pb^{2+} . These results further indicated that the inhibition of AChE by Pb^{2+} follows a reversible mechanism. Moreover, an effect of activation on the catalytic activity of the immobilized AChE was observed. As shown in Fig. 6, the inhibition percentage decrease from 8.64% to 0.78%, which indicated that there exists an activation factor. Researchers have discovered the phenomenon of activation for Fe^{3+} and Mn^{2+} [12,13]. In this work, Fe^{2+} could also present an effect of activation.

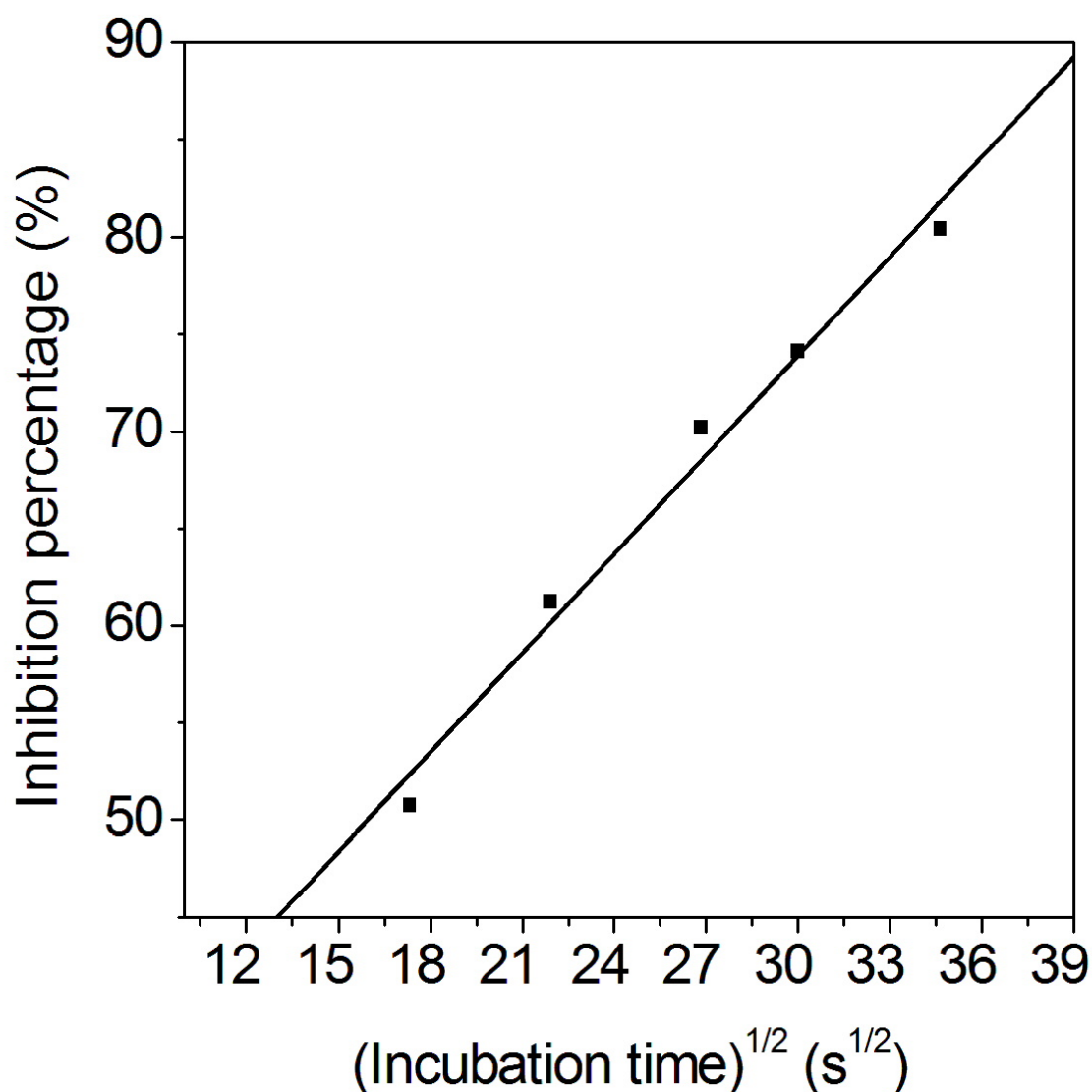


Figure 5. The relationship between inhibition percentage and incubation time for $1 \mu\text{g mL}^{-1}$ malathion.

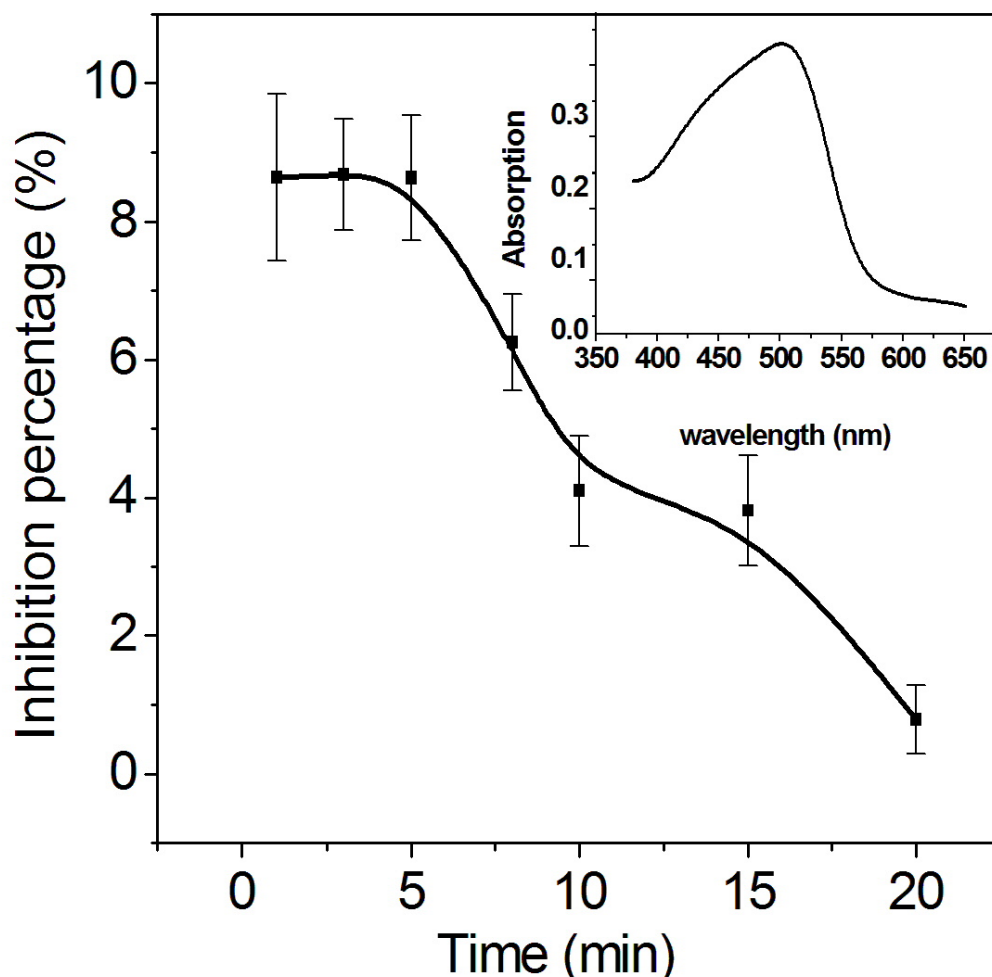


Figure 6. The relationship between inhibition percentage and incubation time for $50 \mu\text{g mL}^{-1} \text{Fe}^{3+}$. Inset: UV-vis absorption spectra of $\text{Fe}(\text{phen})_3^{2+}$ by performing the assay in the PBS containing ATCl and $50 \mu\text{g mL}^{-1} \text{Fe}^{3+}$ after 5 min inhibition. Error bars represent 1 standard deviation for three measurements.

Previous reports have shown that the immobilized AChE mediated hydrolysis of ATCl to yield a reducing agent thiocholine, which led to the enlargement of AuNPs in the present of gold nano-seeds [4,24]. Therefore, with the increase of incubation time, there may present Fe^{2+} in the system consisting of the AChE-AuNPs-SiSG, Fe^{3+} and the substrate ATCl. In the presence of Fe^{3+} , Fe^{3+} can be reduced to Fe^{2+} by thiocholine. To determine whether there exist Fe^{2+} or not, we further carry out UV-vis absorption spectra by performing the assay in the PBS containing ATCl after 5 min inhibition (inset in Fig. 6). The peaks located at 504 nm was identified $\text{Fe}(\text{phen})_3^{2+}$, based on the UV-vis absorption spectra [36]. With these results in hand, we are able to believe that Fe^{2+} presents an effect of activation.

3.5. The relationship between inhibition percentage and inhibitor concentration

The relationship between the inhibition percentage (I%) and the concentration of inhibitor ($[\text{I}]_B$) was also examined. Under the optimal experimental conditions, the inhibition of malathion on

AChE-AuNPs-SiSG/Au was proportional to its concentrations in the range of 0.001 to 1 $\mu\text{g mL}^{-1}$ with the correlation coefficients of 0.998 (Fig. 7). They are in good agreement with the presented above experimental results, illustrating that the percentage of inhibited enzyme (I %), after exposure to an inhibitor, is linearly related to the inhibitor concentration [35].

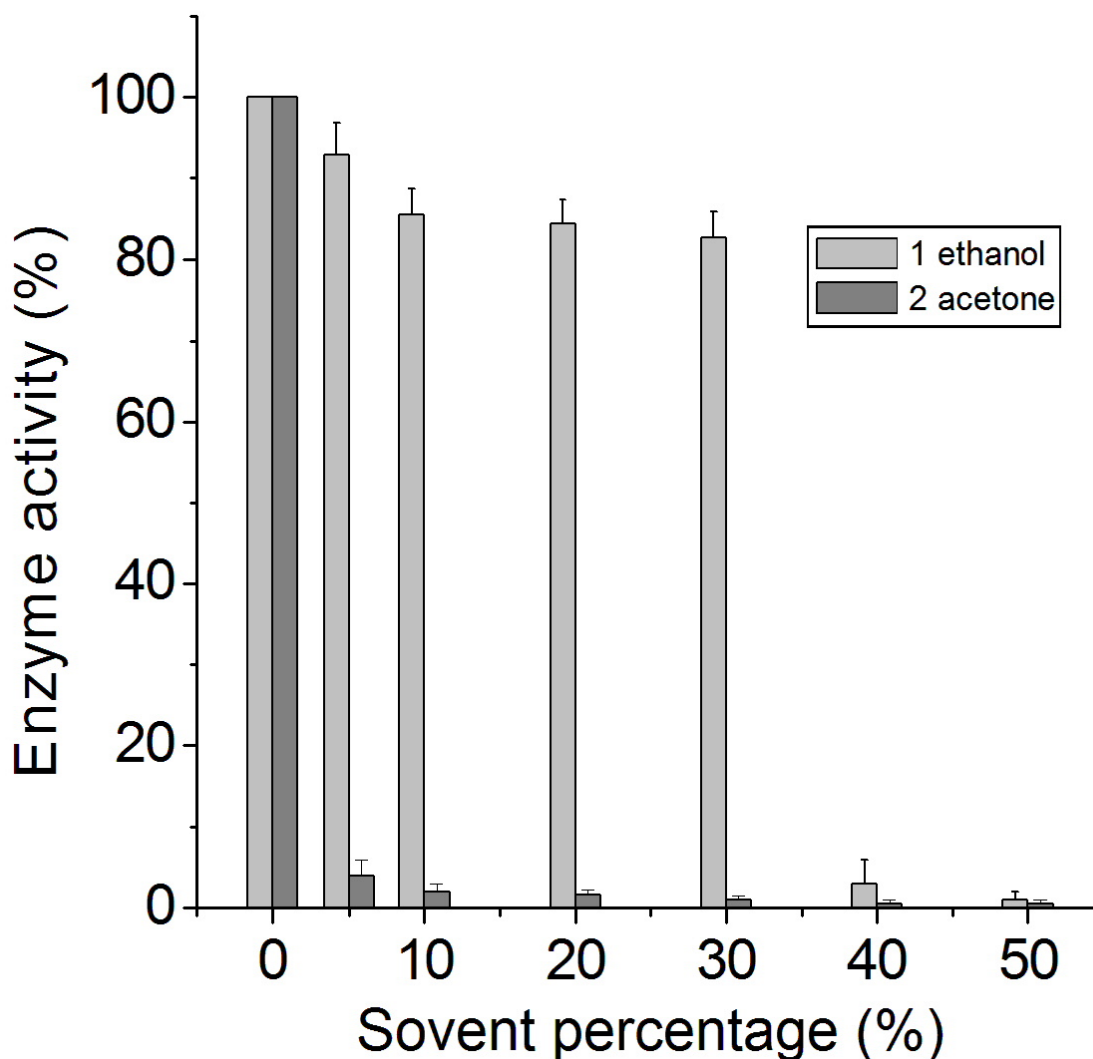


Figure 7. The relationship between inhibition percentage and malathion concentration. Error bars represent 1 standard deviation for three measurements.

3.6. Effect of organic solvent

From a practical point of view, it is important to follow the enzyme's sensitivity to solvent effects. Toward this goal, we investigated the AChE inactivation by acetone and ethanol. Fig. 8 shows that the AChE activity sharply decreased with an increase in the amount of acetone. For 5% (v/v) acetone in phosphate buffer containing 3mM ATCl, the AChE activity decreased by 96%. For ethanol, little inactivation was observed in the range 0-5% ethanol in buffer. Moreover, AChE can maintain its 80% activity using a percentage of ethanol as high as 30%. When it comes to 40%, obvious inhibition can be seen.

However, it is worthy to note that even the highest percentage of acetone or ethanol has no effect on the degree of AChE inhibition by malathion, though this amount of acetone or ethanol in buffer decreased the control level of AChE activity.

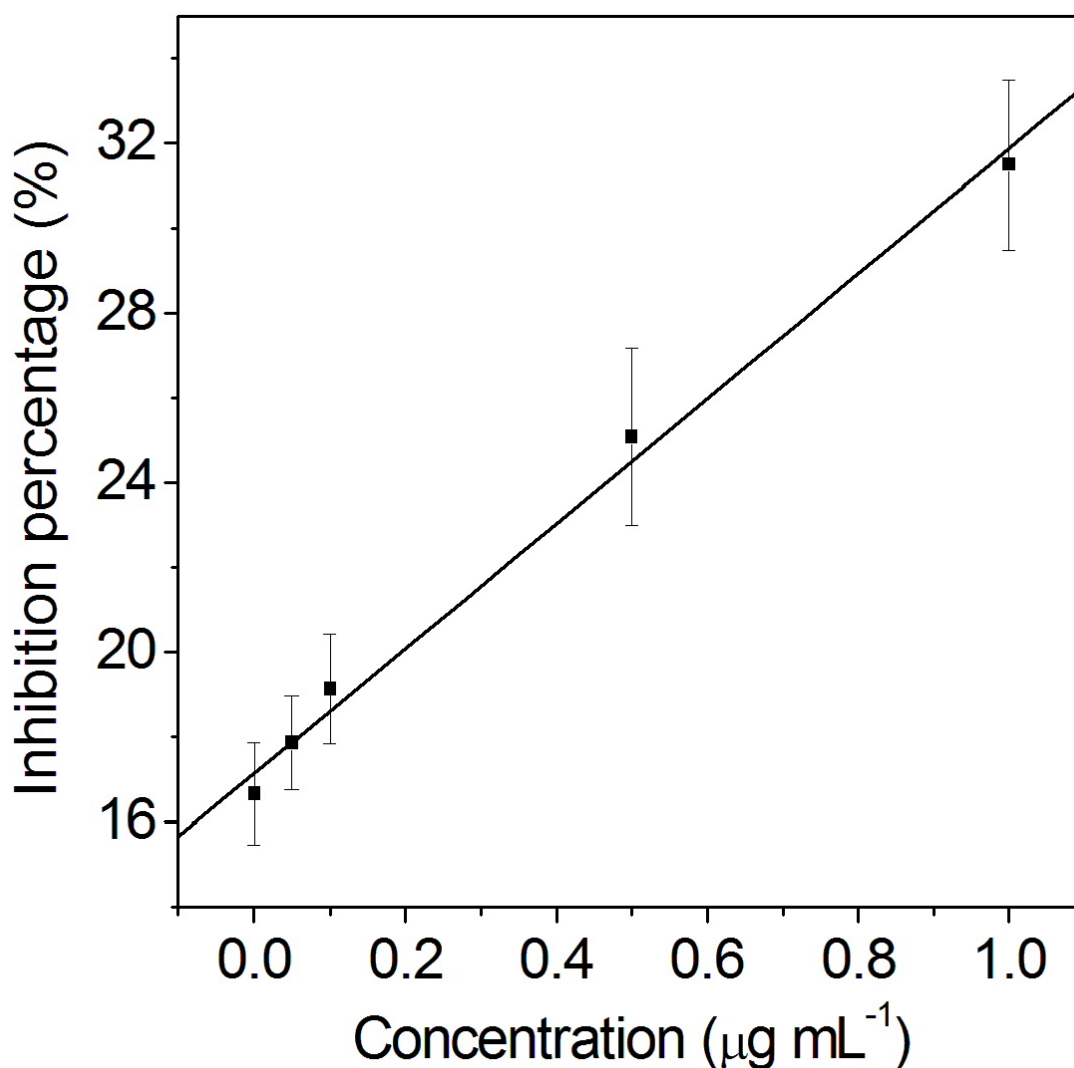


Figure 8. The relationship between the enzyme's sensitivity and solvent concentration of ethanol (1) and (2) acetone. Error bars represent 1 standard deviation for three measurements.

3.7. Reactivation of the biosensor

Fig. 9 shows the photographs of the AChE before (1) and after (2) inhibition of malathion ($1 \mu\text{g mL}^{-1}$) in the presence of 0.5 mM 5, 5'-bithiobis-2-nitrobenzoate (DTNB) and 0.3 mM ATCl. It can be seen that the enzyme activity was inhibited by malathion. Moreover, no absorbance change of the solution was observed after a week (data are not shown). Therefore, we can further confirm that the inhibition of AChE by malathion follows a irreversible mechanism. However, the AChE inhibited irreversibly by organophosphorous pesticides can be completely reactivated using nucleophilic compounds such as pralidoxime iodide. As shown in Fig. 9, AChE inhibited by malathion can resume

96 % original activity after adding 4.0 mM pralidoxime iodide for 10 min. (3 in Fig. 9). As described in our previous research, the nucleophilic compounds capture the enzyme-pesticide complex, which result in the release of free enzyme [20]. Based on this reactivation procedure the proposed biosensor could be repeatedly used with an acceptable reproducibility.



Figure 9. Photograph images of the AChE before (1), after (2) inhibition of malathion ($1 \mu\text{g mL}^{-1}$) and (3) represents reactivation by 4.0 mM pralidoxime iodide for 10 min in the presense of 0.5 mM 5, 5,-bithiobis-2-nitrobenzoate (DTNB) and 0.3 mM ATCl compared with (4) control experiment.

4. CONCLUSIONS

In summary, an electrochemically deposited biointerface was constructed and used to elucidate the chemical mechanism of AChE inhibition. Besides the relationship between inhibition percentage and both incubation time and inhibitor concentration, the enzyme's sensitivity to solvent effects and reactivation of the biosensor were also evaluated. The inhibition of AChE by malathion and metal ions (Pb^{2+} , Fe^{3+}) follows an irreversible and reversible inhibition mechanism respectively. It is envisaged that the present research will be useful for new drugs design and biosensor construction. Moreover, the electrochemical approach could be expanded to other enzyme's mechanism research.

ACKNOWLEDGEMENTS

The authors are gratefully acknowledging the financial support of the National Natural Science Foundation of China (No.21207156) and the Science and Technology Project of Yantai (2012132)

References

1. Y.Q. Miao, N.Y. He and J.J. Zhu, *Chem. Rew.* 110 (2010) 5216.

2. V.B. Kandimalla and H.X. Ju, *Chem. Eur. J.* 12 (2006) 1074.
3. G.D. Liu and Y.H. Lin, *Anal. Chem.* 78 (2006) 835.
4. V. Pavlov, Y. Xiao and I. Willner, *Nano Lett.* 4 (2005) 649.
5. D. Du, J.W. Ding, J. Cai and A.D. Zhang, *Sens. Actuators B-Chem.* 134 (2008) 908.
6. K.L. Vanzolini, L.C.C. Vieira, A.G. Corrêa, C.L. Cardoso and Q.B. Cass, *J. Med. Chem.* 56 (2013) 2038.
7. S. Zhang, H. Zhao and R. John, *Biosens. Bioelectron.* 16 (2001) 1119.
8. M. Bartolini, V. Cavrini and V. Andrisano, *J. Chromatogr. A* 1144 (2007) 102.
9. F. Arduini, I. Errico, A. Amine, L. Micheli, G. Palleschi and D. Moscone, *Anal. Chem.* 79 (2007) 3409.
10. M. Ovalle, M. Stoytcheva, R. Zlatev and B. Valdez, *Electrochim. Acta* 55 (2009) 516.
11. M. Ovalle, M. Stoytcheva, R. Zlatev, B. Valdeza and Z. Velkova, *Electrochim. Acta* 53 (2008) 6344.
12. M. Stoytcheva and V. Sharkova, *Electroanalysis* 14 (2002) 1007.
13. M. Stoytcheva, V. Sharkova and J.P. Magnin, *Electroanalysis* 10 (1998) 994.
14. D. Du, S.Z. Chen, J. Cai and A.D. Zhang, *J. Electroanal. Chem.* 611 (2007) 60.
15. D. Du, S.Z. Chen, J. Cai and A.D. Zhang, *Talanta* 74 (2008) 766.
16. A. Amine, H. Mohammadi, I. Bourais and G. Palleschi, *Biosens. Bioelectron.* 21 (2006) 1405.
17. J. Haccoun, B. Piro, V. NoËl and M.C. Pham, *Bioelectrochemistry* (2006), 68, 218.
18. P.N. Deepa, M. Kanungo, G. Claycomb, P.M.A. Sherwood and M. Collinson, *Anal. Chem.* 75 (2003) 5399.
19. C. Kurzawa, A. Hengstenberg and W. Schuhmann, *Anal. Chem.* 74 (2002) 355.
20. D. Du, J.W. Ding, J. Cai and A.D. Zhang, *J. Electroanal. Chem.* 605 (2007) 53.
21. D. Du, J.W. Ding, J. Cai and A.D. Zhang, *Colloid Surface B.* 58 (2007) 145.
22. M.M. Collinson, N. Moore, P. N. Deepa and M. Kanungo, *Langmuir* 19 (2003) 7669.
23. O. Nadzhafova, M. Etienne and A. Walcarius, *Electrochem. Commun.* 9 (2007) 1189.
24. D. Du, J.W. Ding, J. Cai and A.D. Zhang, *Sens. Actuators B-Chem.* 127 (2007) 317.
25. T. M.B.F. Oliveira, M. Fátima Barroso, S. Morais, M. Araújo, C. Freire, P. de Lima-Neto, A.N. Correia, M.B.P.P. Oliveira and C. Delerue-Matos, *Bioelectrochemistry* 98 (2014) 20.
26. K. Saha, S.S. Agasti, C. Kim, X.N. Li and V.M. Rotello, *Chem. Rev.* 112 (2012) 2739.
27. D. Du, J.W. Ding and J. Cai, A.D. *Talanta* 74 (2008) 1337.
28. D. Du, S.Z. Chen, J. Cai and A.D. Zhang, *Biosens. Bioelectron.* 23 (2007) 130.
29. L.K. Wu and J.M. Hu, *Electrochim. Acta* 116 (2014) 158.
30. H. Schulze, S. Vorlov'a, F. Villatte, T.T. Bachmann and R.D. Schmid, *Biosens. Bioelectron.* 18 (2003) 201-209.
31. E. Suprun, G. Evtugun, H. Budnikov, F. Ricci, D. Moscone and G. Palleschi, *Anal. Bioanal. Chem.* 383 (2005) 597.
32. D.Z. Krstić, M. Čolović, M. Bavcon kralj, M. Franko, K. Krinulović, P. Trebše and V. VASIĆ, *J. Enzym. Inhib. Med. Ch.* 23 (2008) 562.
33. M. Stoytcheva, *Electroanalysis* 14 (2002) 923.
34. G.L. Ellman, K.D. Courtney, V. Andres and R.M. Featherstone, *Biochem. Pharmacol.* 7 (1961) 8.
35. S. Zhang, H. Zhao and R. John, *Electroanalysis* 13 (2001) 1528.
36. Z.O. Tesfaldet, J.F. van Staden and R.I. Stefan, *Talanta* 64 (2004) 1189.